analytical chemistry

Letter

Cite This: *Anal. Chem.* 2020, 92, 573−577

pubs.acs.org/ac

CRISPR/Cas13a Signal Amplification Linked Immunosorbent Assay for Femtomolar Protein Detection

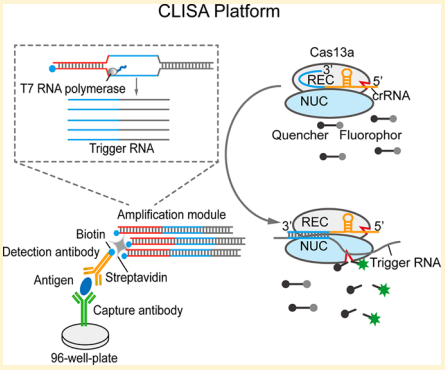
Qian Chen,[†] Tian Tian,[‡] Erhu Xiong,[‡] Po Wang,*[,†] and Xiaoming Zhou*[,‡]

[†]School of Chemistry and Materials Science, Jiangsu Normal University, Xuzhou 221116, China

[‡]School of Life Sciences, South China Normal University, Guangzhou 510631, China

Supporting Information

ABSTRACT: The enzyme-linked immunosorbent assay (ELISA) is a basic technique used in analytical and clinical investigations. However, conventional ELISA is still not sensitive enough to detect ultralow concentrations of biomarkers for the early diagnosis of cancer, cardiovascular risk, neurological disorders, and infectious diseases. Herein we show a mechanism utilizing the CRISPR/Cas13a-based signal export amplification strategy, which double-amplifies the output signal by T7 RNA polymerase transcription and CRISPR/Cas13a collateral cleavage activity. This process is termed the CRISPR/Cas13a signal amplification linked immunosorbent assay (CLISA). The proposed method was validated by detecting an inflammatory factor, human interleukin-6 (human IL-6), and a tumor marker, human vascular endothelial growth factor (human VEGF), which achieved limit of detection (LOD) values of 45.81 fg/mL (2.29 fM) and 32.27 fg/mL (0.81 fM), respectively, demonstrating that CLISA is at least 10^2-fold more sensitive than conventional ELISA.



Downloaded via 58.215.212.98 on April 18, 2026 at 13:39:53 (UTC).
See https://pubs.acs.org/sharingguidelines for options on how to legitimately share published articles.

Immunoassays can be utilized for detecting almost any biomolecules, including proteins, small molecules, vesicles, nucleic acids, and even whole cells.[1,2] Since the invention of this method in the 1960s, immunoassays have undergone a developmental phase from radioimmunoassays to enzyme-linked immunoassays.[3] Using enzymes rather than radioactivity as the reporter label, enzyme-linked immunoassays, also termed enzyme-linked immunosorbent assays (ELISAs), have become the most widely used technique in both fundamental and applied immunological research.[3] With enzymatic signal amplification, ELISA has achieved a limit of detection (LOD) of approximately 0.01−50 ng/mL (pM to nM), depending on the affinity of the antibody.[4] Although it has achieved wide adoption in conventional diagnostic applications, ELISA is still not sensitive enough to detect ultralow concentrations of biomarkers in the early diagnosis of cancer, cardiovascular risk, neurological disorders, and infectious diseases.[5]

To enhance the sensitivity of ELISA, some interesting assay designs were presented. For example, enhancement strategies based on nanoparticles have been extensively reported. One of the representative research studies has focused on the use of nanoparticles for improving the activity of enzymes, such as the exploitation of nanozymes.[6−8] On the other hand, the researchers have explored nanoprobes to load enzymes due to their large specific surface area, which can increase the load of enzyme and achieve signal amplification.[9,10] However, since the nanomaterial is a nonbiological material, it may impair the enzyme activity due to the low biocompatibility. Further, the nonuniformity of the nanoparticle may lead to a great error in measurements. Another promising route to improve the sensitivity of ELISA is the use of nucleic acids-based amplification methods. Instead of using an enzyme, a reporter using a DNA sequence as a signal output can significantly improve the sensitivity of the ELISA method. Typical examples include immuno-PCR,[11−13] immuno-RCA,[14,15] immuno-HCR,[16,17] proximity ligation assays,[18,19] and T7 transcription amplification.[20] As a consequence, the LOD of a given ELISA is, in general, enhanced 10−10^4-fold by the use of DNA as a signal amplification element. Even with these developments, there are still significant challenges for their widespread adoption in analytical and clinical investigations. Possible limiting factors include the inability to achieve quantitative detection due to nonlinear signal amplification, which requires additional testing equipment and detection steps and, thus, is incompatible with existing commercial ELISA platforms.

Recently, CRISPR/Cas13a has been recently demonstrated to have RNA-directed RNA cleavage ability.[21−23] This RNA-guided *trans*-endonuclease activity is highly specific, being activated only when the target RNA has the perfect complementary sequence to the crRNA, and highly efficient (at least 10^4 turnovers per target RNA recognition).[21−23] This potent signal amplification ability of CRISPR/Cas13a enables the development of direct RNA assays with a sensitivity down to the femtomolar level.[21,23,24] Single molecule RNA detection could also be achieved when combined with a digital droplet assay.[25] Although there has been extensive development in

Received: September 27, 2019
Accepted: December 18, 2019
Published: December 18, 2019

© 2019 American Chemical Society

DOI: 10.1021/acs.analchem.9b04403
Anal. Chem. 2020, 92, 573−577

nucleic acid detection, a CRISPR/Cas13a system has not yet been explored as an exciting opportunity for an immunoassay. Since conventional ELISA methods typically only detect biomarkers of picomolar sensitivity levels, it is meaningful to develop a new technique extending the detection sensitivity to the femtomolar range. Due to the highly efficient signal amplification ability, we therefore envisage the application of the CRISPR/Cas13a system to immunoassays and hope to propose a new approach to revolutionize conventional ELISA techniques. Based on the immunological binding mechanism of conventional sandwich structures, we replaced an enzyme (such as horseradish peroxidase) with a biotinylated double-stranded DNA (dsDNA) containing a T7 promoter sequence. T7 polymerase can recognize the promoter sequence to perform the transcription, and many copies of single-stranded RNA molecules are produced. We then designed a CRISPR/Cas13a system to recognize the transcribed RNA molecules, then accurate RNA molecular recognition led to the activation of *trans*-cleavage activity of CRISPR/Cas13. Short ssRNA reporter labeled with fluorophore and quencher groups at both ends of the sequence in the system can be cleaved by the *trans*-cleavage activity. The new version of ELISA performed via using CRISPR/Cas13a as a signal amplification strategy is termed the CRISPR/Cas13a signal amplification linked immunosorbent assay (CLISA). It is the first example, to our knowledge, of the construction of a highly sensitive immunoassay based on the CRISPR/Cas13a system.

The proposed method was validated by detecting an inflammatory factor, human interleukin-6 (human IL-6), and a tumor marker, human vascular endothelial growth factor (human VEGF), which achieved limit of detection (LOD) values of 45.81 fg/mL (2.29 fM) and 32.27 fg/mL (0.81 fM), respectively, demonstrating that CLISA is at least 10^2-fold more sensitive than conventional ELISA.

RESULTS AND DISCUSSION

Recently discovered Cas12, Cas13, and Cas14 systems have certain new features that are different from the Cas9 system. In these systems, recognition of target DNA or RNA leads to their switch to an active state, wherein the single-stranded DNA (ssDNA) or RNA (ssRNA) substrates are cleaved in a nonspecific way. This collateral cleavage activity is termed *trans*-cleavage. Here, we intended to use this target dependent *trans*-cleavage as the signal output mechanism for constructing immunoassay. Among the three systems, the Cas13a system was found to have the highest *trans*-cleavage efficiency, so we chose the Cas13a system for the signal conversion platform for developed CLISA.

As is reported, LbuCas13a has two lobes (REC and NUC).[26] The REC lobe is involved in the cleavage of pre-crRNA. The NUC lobe undergoes a conformational change upon crRNA binding. The formation of the crRNA/target RNA duplex activates HEPN catalytic site of Cas13a. Then, the activated Cas13a cleaves the ssRNA in solution. In this work, a short ssRNA reporter was designed with the modification of FAM and BHQ group at the 5′- and 3′-ends, respectively. Cleavage of this probe leads to a fluorescence enhancement. RNA recognition-dependent ssRNA cleavage constitutes the basis for RNA detection. The crRNAs show a structure of a 5′ forming single hairpin loop (the yellow part in Figure 1A), which is flanked by a 3′ ∼20−30-nt spacer "guide" sequence (the blue part in Figure 1A). Research shows that a

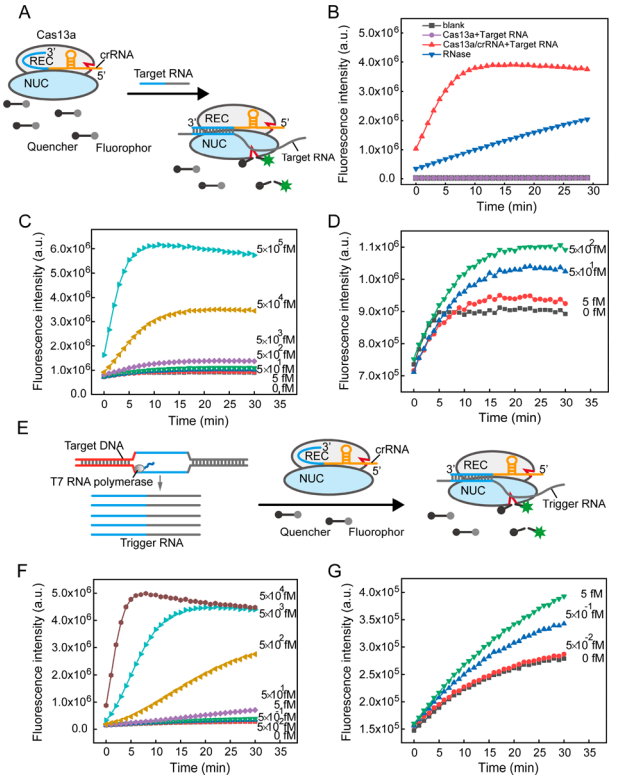


Figure 1. (A) Schematic for the principle of a Cas13a/crRNA-mediated RNA triggered signal amplification system. (B) Fluorescence measurement of LbuCas13a activity. RNase A was used as a positive control for the degradation of the RNA reporter probe. (C) Sensitivity of Cas13a/crRNA-mediated target RNA detection. Real-time fluorescence kinetic measurement of Cas13a reactions initiated by target RNA concentrations from 5 to 5 × 10^5 fM. (D) An enlarged view of the curves at the low concentrations of 0, 5, 50, and 500 fM in part C. Data represent mean ± s.d., n = 3, three technical replicates. (E) Schematic for the principle of a Cas13a/crRNA-mediated RNA triggered signal amplification system after DNA transcription. (F) Sensitivity of Cas13a/crRNA-mediated RNA detection after DNA transcription. Real-time fluorescence kinetic measurement of Cas13a reactions initiated by transcription of DNA concentrations from 5 × 10^{-2} to 5 × 10^4 fM. (G) An enlarged view of the curves at the low concentrations of 0, 5 × 10^{-2}, 5 × 10^{-1}, and 5 fM in part F. Data represent mean ± s.d., n = 3, three technical replicates.

20-nt spacer is sufficient for maximal cleavage activity for LbuCas13a.[27,28]

Prior to carrying out the CLISA, the collateral cleavage activity of CRISPR/Cas13a and the sensitivity of detecting the RNA were first demonstrated. The CRISPR/Cas13a cleavage mechanism is shown in Figure 1A. Cas13a exhibits high activity under the guidance of crRNA in the presence of a synthesized target RNA. As shown in Figure 1B, the collateral cleavage activity of Cas13a can only be activated when Cas13a/crRNA/target RNA are present simultaneously (red curve). After that, we performed the CRISPR/Cas13a assay for RNA detection. As shown in Figure 1C, with the increase of target RNA concentrations, the fluorescence signals enhanced gradually, and the CRISPR/Cas13a system was able to detect the target RNA at as low of a concentration of 50 fM. Figure 1D shows an enlarged view of the low concentration measurement curve in Figure 1C. Direct detection of RNA at a femtomolar sensitivity level without a target RNA amplification indicates that the Cas13a system is one of the

DOI: 10.1021/acs.analchem.9b04403
Anal. Chem. 2020, 92, 573−577

most sensitive detection assays currently known. We therefore envisage that such a sensitivity is enough for developing a highly sensitive immunoassay. We chemically synthesized a biotinylated RNA as a signal output for the Cas13a-based immune detection system. The biotinylated RNA is added to the immune-complex for linking secondary antibody by streptavidin. After washing, the analytical performance of the Cas13a-based detection system is evaluated.

Unexpectedly, experimental results have shown that the detection efficiency is very low. We judge that this may be caused by two reasons. One is the steric-hindrance effect. Cas13a/crRNA is a large complex with a molecular weight of more than 200 kDa, so its contact with the biotinylated RNA, which is linked to antibody−antigen−antibody−streptavidin complex may be less effective. The other reason is that when the biotinylated RNA is fixed onto the ELISA plate after binding to the secondary antibody, this heterogeneous reaction can also cause lower efficiency than that of the homogeneous reaction. Therefore, we introduced the transcription process before the CRISPR/Cas13a assay, using T7 promoter tagged DNA instead of RNA to improve detection efficiency of the Cas13a assay and to avoid any instability problem during the procedure of incubation and washing. As shown in Figure 1E, the T7 transcription process was added prior to the CRISPR/Cas13a assay. The results show that CRISPR/Cas13a is capable of detecting DNA transcripts at concentrations as low as 500 aM (as shown in Figure 1F,G), and Figure 1G presents an enlarged view of the low concentration curve in Figure 1F. The LOD of post-transcriptional detection was enhanced by 2 orders of magnitude compared to direct RNA detection.

We observed that in Figure 1C,D, the detection signal reached a stable plateau after 10 min. While in all the measured concentrations in Figure 1F,G (even if the target concentration is 0), the detection signal shows a continuous increasing trend. Note that Figure 1C,D shows the direct detection of chemically synthesized RNA targets using the Cas13a system, while Figure 1F,G show the detection of T7 polymerase transcription products. One possible reason for the increased background signals is the T7 polymerase transcription mechanism, where T7 polymerase was not inactivated in the system, so transcription was not terminated during the Cas13a assay, resulting in a sustained increase in signal. Another possible explanation is the complex reaction system (Cas13a protein, crRNA, T7 polymerase, NTPs, and buffer) causes a faint hydrolysis of the RNA probe. Fortunately, our experiments still demonstrate that T7 transcription leads to increased sensitivity when compared to direct detection of RNA target molecules (Figure S3A,B). As shown in Figure 1D,G, we also show the results of the 5 fM RNA target in the direct detection method and the 5 fM DNA template in the T7 polymerase-based method. Obviously, T7 transcription leads to an enhancement in sensitivity.

The achieved impressive sensitivity enabled us to construct a new ELISA built on the basis of a transcription assisted CRISPR/Cas13a assay. As is well-known, classical ELISA is a heterogeneous assay format using a solid phase well plate. We next proved the feasibility of utilizing DNA transcription for this purpose by using a 96-well plate. As shown in Figure 2A, streptavidin was used to directly coat the 96-well plates, and then the plates were blocked with 1% BSA protein. A biotinylated DNA amplification template containing a T7 promoter sequence at one end was then added to the plate. Then, the unbound DNA amplification template was removed

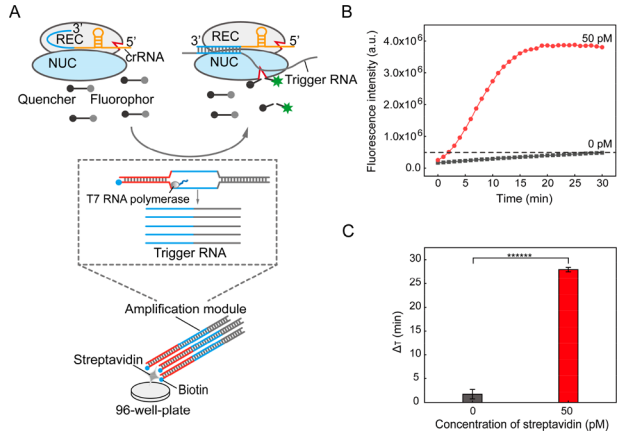


Figure 2. Validation of the compatibility of the Cas13a/crRNA-mediated RNA detection system with solid phase DNA transcription. (A) Streptavidin was precoated on a 96-well plate. The biotin-dsDNA amplification template (the amplification module) then bound to the streptavidin. The bound biotin-dsDNA was used as the template for DNA transcription by T7 RNA polymerase. (B) Real-time fluorescence kinetic measurement of simplified CLISA. The threshold was set to determine the critical time τ, which is the minimal time to reach the threshold. A calibration curve was then established by plotting $\Delta\tau$ ($\Delta\tau$ = 30 min − τ) as a function of the concentrations of streptavidin (C) (Student's t test; ******P < 0.00001). Data represent mean ± s.d., n = 3, three technical replicates.

by washing. Next, transcription reaction buffer, T7 RNA polymerase, and nucleotide triphosphates (NTPs) were mixed together and transcribed at 37 °C for 1 h. Finally, the transcription products were detected by CRISPR/Cas13a. The fluorescence kinetic curves of each well were recorded, and the fluorescence intensity increased at 50 pM of template DNA (Figure 2B, red curve). In addition, the results were also expressed by the calibration values ($\Delta\tau$) in Figure 2C. In the presence of 50 pM template DNA, the $\Delta\tau$ value was much stronger than that of the negative control, indicating that the template DNA was successfully ligated to the plate and the DNA transcript can be successfully detected in a solid phase format.

After demonstrating a solid phase transcription assisted CRISPR/Cas13a assay, CLISA was developed. We chose human IL-6 and human VEGF as models to validate the CLISA. Human IL-6 is an inflammatory factor produced by tumor cells, T cells, and lymphocytes.[29,30] Human VEGF is involved in the pathogenesis and progression of many angiogenesis-dependent diseases, including cancer, certain inflammatory diseases, and diabetic retinopathy.[31] Human IL-6 and human VEGF have been considered to be important factors in disease development.

First, we applied CLISA to detect human IL-6. Serially diluted human IL-6 antigen and biotinylated detection antibody were added sequentially to form "antibody−antigen−antibody" complexes. After that, streptavidin and the biotinylated DNA amplification template, which has been optimized as shown in Figure S4, were added sequentially, resulting in binding of the DNA amplification template to the "antibody−antigen−antibody" complex. Unbound templates were washed away, and then T7 RNA polymerase was utilized to amplify the amplification template (Figure 3A). In the CLISA, antigen−antibody binding, template transcription and Cas13a detection were all performed at 37 °C. As shown in

DOI: 10.1021/acs.analchem.9b04403
Anal. Chem. 2020, 92, 573−577

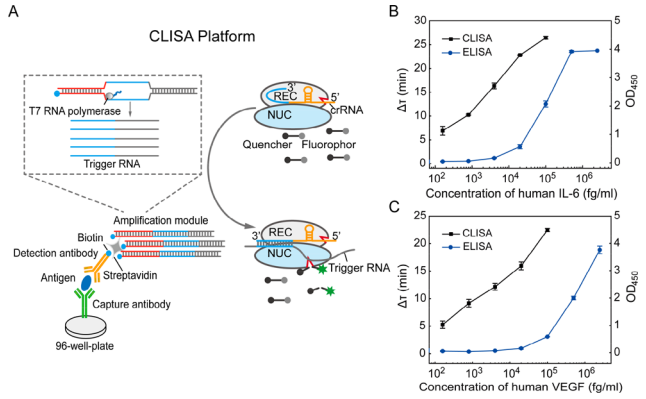


Figure 3. (A) Schematic for the principle of CLISA. In a CLISA assay, the capture antibody first binds to the antigen of interest. A detection antibody, which binds to a distant, nonoverlapping epitope in the antigen, is biotinylated and linked to a biotin-dsDNA template (the amplification module) through streptavidin. T7 RNA polymerase is then used to amplify the DNA template, producing many copies of RNA substrate, the amount of which is representative of the original amount of antigen. (B) Detection of human IL-6. Human IL-6 was added to the coated plate at a series of 5-fold dilutions from 160 fg/mL (8 fM) to 100 pg/mL (5 pM). A calibration curve was established by plotting $\Delta\tau$ as a function of the concentrations of human IL-6. A parallel ELISA experiment was also performed with a series of 5-fold dilutions from 160 fg/mL (8 fM) to 2.5 ng/mL (125 pM). Data represent mean ± s.d., n = 3, three technical replicates. (C) Detection of human VEGF. Human VEGF was added to the coated plate at a series of 5-fold dilutions from 160 fg/mL (4 fM) to 100 pg/mL (2.5 pM). A calibration curve was established by plotting $\Delta\tau$ as a function of the concentrations of human VEGF. A parallel ELISA experiment was also performed at a series of 5-fold dilutions from 160 fg/mL (4 fM) to 2.5 ng/mL (62.5 pM). Data represent mean ± s.d., n = 3, three technical replicates.

Figure 3B, it is noted that the $\Delta\tau$ is linear with the logarithm of human IL-6 concentrations in the range from 160 fg/mL (8 fM) to 0.1 ng/mL (5 pM), and the linear regression equation is $\Delta\tau = 8.496 \lg C - 14.112$ ($R^2 = 0.989$) with a LOD of 45.81 fg/mL (2.29 fM). In addition, a commercial human IL-6 ELISA kit was subjected to the same experiment and showed a LOD of 12.09 pg/mL (605 fM) (blue curve). It is significant that the sensitivity of CLISA was 264-fold higher than that of the commercial ELISA kit.

In addition, as displayed in Figure 3C, we also applied CLISA to detect human VEGF. In the range of 160 fg/mL (4 fM) to 0.1 ng/mL (2.5 pM) of human VEGF, there is a linear relationship between the $\Delta\tau$ and the logarithm of human VEGF concentrations, with a linear regression equation of $\Delta\tau = 6.347 \lg C - 9.577$ ($R^2 = 0.985$) and a LOD as low as 32.27 fg/mL (0.81 fM). The commercial ELISA human VEGF kit showed an LOD of 20 pg/mL (500 fM) (Figure 3C). This result indicated that the LOD of the CLISA was also reduced by 617-fold compared to the commercial ELISA kit.

Next, we evaluated the detection precision data and analytical potential of the proposed CLISA method for complex samples. The precision of CLISA was evaluated by analyzing three concentrations (100, 20, and 4 pg/mL) of human IL-6. The relative standard derivations (RSD, n = 8) of the detection signals for these three concentrations are 1.35%, 2.33%, and 6.50%, respectively. Then, we added human IL-6 to 20% and 100% mouse serum, respectively, to demonstrate whether the CLISA method is as resistant to matrix interference as a conventional ELISA method. The recovery test evaluating from three concentrations (100, 20, and 4 pg/mL) of human IL-6 samples showed that the recoveries were 96.21%, 101.30%, and 104.25%, respectively, for 20% serum samples, and 83.59%, 94.90%, and 94.25%, respectively, for 100% serum samples (Table 1). Since the procedure of the

Table 1. Recovery Experiments of Human IL-6 in Serum Samples

	20% serum		100% serum	
spiked conc (pg/mL)	mean ± SD (pg/mL)	recovery (%)	mean ± SD (pg/mL)	recovery (%)
100	96.21 ± 7.03	96.21	83.59 ± 4.03	83.59
20	20.26 ± 4.20	101.30	18.98 ± 1.20	94.90
4	4.17 ± 3.90	104.25	3.77 ± 0.34	94.25

current CLISA method requires washing similar to the conventional ELISA method, it is not surprising that the CLISA method has achieved an excellent anti-interference ability.

Compared with the traditional ELISA, CLISA adds a transcription process to amplify the DNA template, and the signal is further enhanced by the collateral cleavage activity of CRISPR/Cas13a. As a result, the sensitivity of CLISA can be effectively ameliorated by two-step amplification. Furthermore, the whole process of the CLISA is performed at 37 °C, which is an isothermal process without the need for a thermal cycling program. It is worth noting that the CLISA procedure is completely compatible with existing commercial ELISA equipment.

Although the experiments herein were performed manually, it is obvious that this method is compatible with current high-throughput liquid handling robots for washing plates and reagent dispersion. Due to its improved sensitivity over commercial ELISA kits and its adaptability to high-throughput and automation technologies, CLISA can be applied to detect low-abundance proteins that conventional ELISA cannot. In addition, we compared CLISA with several other immunological methods (Table S2). This work shows that the CLISA method is superior in sensitivity to most of the reported amplification strategies. Among these the T7 transcription amplification assay reports a better sensitivity; however, the CLISA method demonstrates superior linearity and speed.

Although this work proposes a new immunoassay concept and achieves excellent detection performance, the limitations are still present when compared to conventional ELISA methods. We think that one of the main problems at present is the stability of the probe. The CLISA method uses a fluorescent and quencher groups-labeled RNA reporter as a signal output, so the detection system needs to be an RNase-free environment in order to avoid reporter degradation, thereby interfering with the experimental results. One of the potential solutions would be to the employment of RNA modifications (such as 2′-O-methoxyethyl and fluorine modification) to avoid potential degradation of the RNA reporter.

■ CONCLUSIONS

In summary, we developed a highly sensitive, isothermal method for detecting low-abundance proteins based on the collateral cleavage activity of CRISPR/Cas13a initiated by trigger RNA. The sensitivity of CLISA was effectively improved by the amplification of T7 transcription and the

DOI: 10.1021/acs.analchem.9b04403
Anal. Chem. 2020, 92, 573−577

collateral cleavage activity of CRISPR/Cas13a. Using human IL-6 and human VEGF as model analytes, the sensitivity of CLISA has been drastically boosted, with a LOD as low as 45.81 fg/mL (2.29 fM, 264-fold improvement) and 32.27 fg/mL (0.81 fM, 617-fold improvement) compared to commercialized ELISA kits. Moreover, the method is compatible with automated and high-throughput format that allows for rapid screening of large numbers of samples simultaneously, providing potential ultrasensitive detection methods for biosensing, medical research, and molecular diagnostics.

■ ASSOCIATED CONTENT

Supporting Information

The Supporting Information is available free of charge at https://pubs.acs.org/doi/10.1021/acs.analchem.9b04403.

Materials and apparatus; experimental methods; Table S1, sequences used in this study; Table S2, comparison of protein test results across published reports; Figures S1 and S2, PAGE gels; Figure S3, calibration curves; and Figure S4, optimization of the streptavidin concentration and biotin dsDNA template concentration (PDF)

■ AUTHOR INFORMATION

Corresponding Authors

*E-mail: wangpo@jsnu.edu.cn.
*E-mail: zhouxm@scnu.edu.cn.

ORCID

Po Wang: 0000-0001-6590-2169
Xiaoming Zhou: 0000-0001-5597-4804

Notes

The authors declare no competing financial interest.

■ ACKNOWLEDGMENTS

We thank Professor Yanli Wang for supplying the plasmid for LbuCas13a expression. This work was supported by the National Natural Science Foundation of China (Grants 91959128, 21475048, 21874049, 21904042, 21675067, and 21205052), the National Science Fund for Distinguished Young Scholars of Guangdong Province (Grant 2014A030306008), the Natural Science Foundation of Jiangsu Province (Grant BE2019645), and the Foundation of Postgraduate Research and the Practical Innovation Program of Jiangsu Normal University (Grant 2018YXJ124).

■ REFERENCES

(1) Wild, D. *The Immunoassay Handbook*, 4th ed.; Elsevier Science: Amsterdam, The Netherlands, 2013.
(2) Han, K. N.; Li, C. A.; Seong, G. H. *Annu. Rev. Anal. Chem.* **2013**, *6*, 119−141.
(3) Lequin, R. M. *Clin. Chem.* **2005**, *51*, 2415−2418.
(4) Dixit, C. K.; Vashist, S. K.; O'Neill, F. T.; O'Reilly, B.; MacCraith, B. D.; O'Kennedy, R. *Anal. Chem.* **2010**, *82*, 7049−7052.
(5) De La Rica, R.; Stevens, M. M. *Nat. Nanotechnol.* **2012**, *7*, 821−824.
(6) Duan, D.; Fan, K.; Zhang, D.; Tan, S.; Liang, M.; Liu, Y.; Zhang, J.; Zhang, P.; Liu, W.; Qiu, X.; Kobinger, G. P.; Fu Gao, G.; Yan, X. *Biosens. Bioelectron.* **2015**, *74*, 134−141.
(7) Gao, L.; Zhuang, J.; Nie, L.; Zhang, J.; Zhang, Y.; Gu, N.; Wang, T.; Feng, J.; Yang, D.; Perrett, S.; Yan, X. *Nat. Nanotechnol.* **2007**, *2*, 577−583.
(8) Yu, Z.; Tang, Y.; Cai, G.; Ren, R.; Tang, D. *Anal. Chem.* **2019**, *91*, 1222−1226.
(9) Thaxton, C. S.; Elghanian, R.; Thomas, A. D.; Stoeva, S. I.; Lee, J. S.; Smith, N. D.; Schaeffer, A. J.; Klocker, H.; Horninger, W.; Bartsch, G.; Mirkin, C. A. *Proc. Natl. Acad. Sci. U. S. A.* **2009**, *106*, 18437−18442.
(10) Jiao, L.; Yan, H.; Xu, W.; Wu, Y.; Gu, W.; Li, H.; Du, D.; Lin, Y.; Zhu, C. *Anal. Chem.* **2019**, *91*, 8461−8465.
(11) Sano, T.; Smith, C. L.; Cantor, C. R. *Science* **1992**, *258*, 120−122.
(12) Niemeyer, C. M.; Adler, M.; Wacker, R. *Nat. Protoc.* **2007**, *2*, 1918−1930.
(13) Sims, P. W.; Vasser, M.; Wong, W. L.; Williams, P. M.; Meng, Y. G. *Anal. Biochem.* **2000**, *281*, 230−232.
(14) Niemeyer, C. M.; Adler, M.; Wacker, R. *Trends Biotechnol.* **2005**, *23*, 208−216.
(15) Schweitzer, B.; Roberts, S.; Grimwade, B.; Shao, W.; Wang, M.; Fu, Q.; Shu, Q.; Laroche, I.; Zhou, Z.; Tchernev, V. T.; Christiansen, J.; Velleca, M.; Kingsmore, S. F. *Nat. Biotechnol.* **2002**, *20*, 359−365.
(16) Zhang, B.; Liu, B.; Tang, D.; Niessner, R.; Chen, G.; Knopp, D. *Anal. Chem.* **2012**, *84*, 5392−5399.
(17) Choi, J.; Routenberg Love, K.; Gong, Y.; Gierahn, T. M.; Love, J. C. *Anal. Chem.* **2011**, *83*, 6890−6895.
(18) Fredriksson, S.; Gullberg, M.; Jarvius, J.; Olsson, C.; Pietras, K.; Gústafsdóttir, S. M.; Östman, A.; Landegren, U. *Nat. Biotechnol.* **2002**, *20*, 473−477.
(19) Gullberg, M.; Gustafsdottir, S. M.; Schallmeiner, E.; Jarvius, J.; Bjarnegard, M.; Betsholtz, C.; Landegren, U.; Fredriksson, S. *Proc. Natl. Acad. Sci. U. S. A.* **2004**, *101*, 8420−8424.
(20) Zhang, H.; Cheng, X.; Richter, M.; Greene, M. I. *Nat. Med.* **2006**, *12*, 473−477.
(21) Gootenberg, J. S.; Abudayyeh, O. O.; Lee, J. W.; Essletzbichler, P.; Dy, A. J.; Joung, J.; Verdine, V.; Donghia, N.; Daringer, N. M.; Freije, C. A.; Myhrvold, C.; Bhattacharyya, R. P.; Livny, J.; Regev, A.; Koonin, E. V.; Hung, D. T.; Sabeti, P. C.; Collins, J. J.; Zhang, F. *Science* **2017**, *356*, 438−442.
(22) Abudayyeh, O. O.; Gootenberg, J. S.; Konermann, S.; Joung, J.; Slaymaker, I. M.; Cox, D. B.; Shmakov, S.; Makarova, K. S.; Semenova, E.; Minakhin, L.; Severinov, K.; Regev, A.; Lander, E. S.; Koonin, E. V.; Zhang, F. *Science* **2016**, *353*, aaf5573.
(23) East-Seletsky, A.; O'Connell, M. R.; Knight, S. C.; Burstein, D.; Cate, J. H.; Tjian, R.; Doudna, J. A. *Nature* **2016**, *538*, 270−273.
(24) Shan, Y.; Zhou, X.; Huang, R.; Xing, D. *Anal. Chem.* **2019**, *91*, 5278−5285.
(25) Tian, T.; Shu, B.; Liu, L.; Zhou, X. *bioRxiv* **2019**, 748939.
(26) Liu, L.; Li, X.; Wang, J.; Wang, M.; Chen, P.; Yin, M.; Li, J.; Sheng, G.; Wang, Y. *Cell* **2017**, *168*, 121−134.
(27) O'Connell, M. R. *J. Mol. Biol.* **2019**, *431*, 66−87.
(28) Knott, G. J.; East-Seletsky, A.; Cofsky, J. C.; Holton, J. M.; Charles, E.; O'Connell, M. R.; Doudna, J. A. *Nat. Struct. Mol. Biol.* **2017**, *24*, 825−833.
(29) Rotter, V.; Nagaev, I.; Smith, U. *J. Biol. Chem.* **2003**, *278*, 45777−45784.
(30) Sansone, P.; Storci, G.; Tavolari, S.; Guarnieri, T.; Giovannini, C.; Taffurelli, M.; Ceccarelli, C.; Santini, D.; Paterini, P.; Marcu, K. B.; Chieco, P.; Bonafè, M. *J. Clin. Invest.* **2007**, *117*, 3988−4002.
(31) Salven, P.; Lymboussaki, A.; Heikkilä, P.; Jääskela-Saari, H.; Enholm, B.; Aase, K.; von Euler, G.; Eriksson, U.; Alitalo, K.; Joensuu, H. *Am. J. Pathol.* **1998**, *153*, 103−108.

DOI: 10.1021/acs.analchem.9b04403
Anal. Chem. 2020, 92, 573−577